International Transaction Journal of Engineering, Management, & Applied Sciences & Technologies

http://TuEngr.com, http://go.to/Research

Experimental and Numerical Investigation of Shock/Turbulence Interaction by Hot-wire Technique

Mohammad Ali Jinnah[a*]

[a] *Mechanical and Chemical Engineering Department, Islamic University of Technology, Board Bazar, Gazipur-1704, BANGLADESH*

ARTICLE INFO

Article history:
Received 23 January 2012
Received in revised form 15 April 2012
Accepted 16 April 2012
Available online 17 April 2012

Keywords:
Shock Wave,
Turbulence,
Hot-wire,
Turbulence grid,
Length Scale

ABSTRACT

In the present paper, an experimental investigation has been carried out to observe the amplification of turbulence intensity after shock/turbulence interaction by hot-wire technique. The hot wires are installed in the wake of turbulent grids to measure turbulence fluctuations before and after the reflected shock interaction with turbulence. It is observed that the turbulence fluctuations for less open area of the grid plate are higher than the turbulence fluctuations for more open area of the grid plate. For numerical computations, grid plate of 49.5 % open area is used. The average longitudinal velocity line obtained from experimental velocity data simulates with numerical results properly and in some places, 5-7 % deviations are observed with numerical results. All the simulation results indicate that the present code with turbulence model is working properly. The substantial amplification of pressure fluctuations obtained from experiment is observed after interaction. The dissipation rate of turbulent kinetic energy (TKE) and the levels of length scales are determined numerically. It is observed that the dissipation rate of TKE and the levels of length scales decrease after shock/turbulence interaction.

*Corresponding author (M. A. Jinnah). E-mail addresses: shahjin2001@yahoo.com.

1. Introduction

The present experimental study has been focused on the measurement of turbulence intensity in the grid-generated turbulent fields by hot-wire technique. The output voltages of the hot-wire anemometer are used to establish the relationship between the hot-wire output voltage and the mean flow velocity. Due to different grid plates, different strengths of turbulent field are observed behind the transmitted shock wave. The turbulence fluctuations in the wake of grid plate are measured experimentally by using hot-wire anemometer.

Experiments on the interaction between the shock wave and the grid-generated turbulence were conducted by Devieve and Lacharme [1] and they measured velocity and temperature spectra upstream and downstream of the shock wave and concluded that turbulent fluctuations were amplified and Taylor micro scales increased during the interaction. Jacquin et al [2] investigated the interactions of a normal shock wave with the grid-generated turbulence and a turbulent jet and they observed that turbulence amplification was not significant for the grid-generated turbulence and that the decay of turbulent kinetic energy was accelerated downstream of the shock wave. Their experiments treated the interaction of a shock with quasi-incompressible turbulence where fluctuations in pressure and density were not significant. They observed that the data obtained from grid-generated turbulence were not sufficient to characterize the turbulence properly. They analyzed the flow by means of laser Doppler velocimetry. The obtained supersonic flow was shocked by means of a second throat creating a pure normal shock wave/free turbulence interaction. On other hand, Devieve and Lacharme [1] obtained a quasi-homogeneous turbulence by generating perturbations in the settling chamber of a supersonic wind tunnel at Mach 2.3. They showed that, after the expansion in the nozzle, the turbulent field became strongly non-isotropic and that the turbulence level was drastically decreased leading to experimental difficulties. Debieve et al [3] analyzed the evolution of turbulence through a shock, and separated the effects of the specific turbulent sources from the effects of the mean motion-convection and production. Their prediction of the longitudinal velocity fluctuation was in good agreement with the experimental results. An experimental work was performed on the interaction of weak shocks (M_s=1.007, 1.03 and 1.1) with a random medium of density in homogeneity by Hesselink and Sturtevant [4]. They observed that the pressure histories of the distorted shock waves were both peaked and rounded and explained these features in terms of the focusing/defocusing of the shock front due to inhomogeneity of the medium. Lele et al [5] conducted direct numerical simulations of two-dimensional turbulence interacting with a shock wave and found that vorticity amplification compared well with the predictions of the linear analysis but turbulent kinetic energy evolution behind the shock showed significant nonlinear effects. The energy spectrum was found to be enhanced more at large wave numbers, leading to an overall length scale decrease. Many researchers used many techniques to measure the turbulence. In the present technique, hot wire anemometer is used to measure the turbulence before and after the shock/turbulence interaction and the results are simulated with numerical results.

2. Experimental Setup

In the present experiment, a vertical shock tube of square cross-section, shown in Figure 1 (i), is used and the square cross-section is 300 x 300 *(mm)*. Four krystler-type pressure transducers are used to measure the pressure history. Above the turbulence grids, two pressure transducers are setup 400 *mm* apart to measure the incident shock strength and the sensitivity of these transducers are 4.98 *pC/bar* and 5.50 *pC/bar*. Another two pressure transducers (P2 and P1) are placed in the wake of the turbulence grids to measure the pressure history in the turbulent field and the distance between the pressure ports P2 and P1 is 560 *mm*. The sensitivity of the pressure transducer at P2 is 4.99 *pC/bar* and the sensitivity of the pressure transducer at P1 is 5.16 *pC/bar*. The distance between the end wall and the turbulence grid is 1000 *mm* and in this distance two hot-wire sensors are placed 560 *mm* apart to measure the turbulence fluctuations. One hot wire is placed near port P2 and second hot wire is placed near port P1 and they are all used to measure the turbulence parameters before and after the interaction. The hot wire contains 1-D hot-wire probe which is used to measure the 1-D flow velocity. A 5-μm wire is spot welded on the probe. The length to diameter ratio of the hot wire is approximately 300. The hot-wire probe is connected to a DANTEC type 55P11 anemometer. To generate the turbulence in the wake of the turbulence grid plate, two types of turbulence grid plates are used in this experiment, which are shown in Figure 2 (i) and (ii). The opening areas of different turbulence grid plates are 66.7 *%* and 49.5 *%*.

The output data of the hot-wire anemometer is in electric voltages. So it is necessary to convert the voltage data to velocity. The relationship between the CTA output E and the velocity U represents the probe calibration, from which the transfer function $U = f(E)$ is

*Corresponding author (M. A. Jinnah). E-mail addresses: shahjin2001@yahoo.com.

derived. The usual functional relation between the Nusselt and Reynolds numbers for the hot wire probe leads to the following expression:

$$\frac{E^2}{T_w - T_o} = A\left(\frac{T_o}{T_r}\right)^a + B\left(\frac{T_o}{T_r}\right)^b (\rho U)^n \tag{1}$$

where T_w is the wire temperature, T_o is the total temperature of the fluid and T_r is the reference temperature. The above equation is suitable for the calibration where the temperature compensation is considered. Honkan and Andreopoulos [6] were conducted experiments to measure the outcomes of shock/turbulence interaction where temperature compensation was considered. It is found that the effect of temperature fluctuations on velocity statistics is very low. So the simplified equation for homogeneous and isotropic turbulence without considering any temperature compensation is as follows:

$$E^2 = A' + B' U^n \quad \textit{(king's law)} \qquad (2),$$

where the values A', B' and the exponent n have to be determined by a suitable calibration procedure. The experiment is conducted for different shock Mach numbers where no grid is used and the shock induced flow velocity *(U)* behind the shock wave can be determined by any one of the two processes. Many researchers were used Laser Doppler velocimeter to measure the longitudinal velocity behind the shock wave. In the present experiment, the shock induced flow velocity *(U)* behind the shock wave is calculated by using Rankine-Hugoniot relations. For different incident shock Mach numbers, the induced flow velocities are determined for the calibration and at the same time, hot-wire data is also recorded for different incident shock Mach numbers and the measured incident shock Mach number is 1.56. Many researchers established the relationship between the output voltage *(E)* and the longitudinal velocity *(U)* to calculate the turbulence intensity of the flow. After solving from different data of *(E, U),* the value of A' = 0.12, B' = 0.17 and n = 0.45. Here the recommended value of n is 0.45, which is a good starting value for wire probes.

(i) 

(ii) 

Figure 1: **(i)** Test section of the vertical shock tube;
(ii) Relative position of the hot wire port and the pressure port at P2 and P1.

(i) 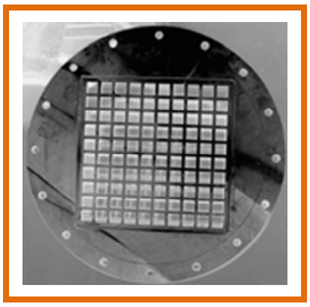
(ii) 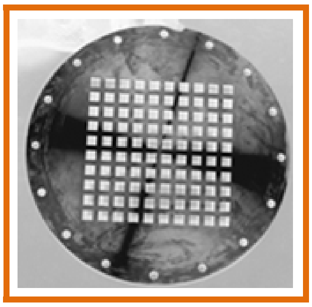

Figure 2: **(i)** Turbulence grid plate of 66.7 % opening area;
(ii) Turbulence grid plate of 49.5 % opening area.

3. Numerical Setup and Specifications

The turbulence grid plate of 49.5 % opening area, shown in Figure 3 (i) and (ii), has been considered a case study of numerical simulation. The model is symmetry for the square cross section so it can easily consider the $1/4^{th}$ part of the cross sectional area of the shock tube for the computational domain. The total length of the domain is 1150 *mm* and 11000 cells are used in this domain for getting good numerical results and the computational domain with turbulence-generating grids is shown in Figure 4. All flow parameters are computed by solving the three dimensional Navier-Stokes equations with k-ε turbulence model.

The three-dimensional unsteady, compressible, Reynolds-averaged Navier-stokes (RANS) equations with k-ε turbulence model are solved by shock capturing method. Without external forces and heat sources, the conservative form of non-dimensionalized governing equation in three-dimensional Cartesian coordinate system is,

*Corresponding author (M. A. Jinnah). E-mail addresses: shahjin2001@yahoo.com.

Volume 3 No.2 ISSN 2228-9860 eISSN 1906-9642. Online Available at http://TuEngr.com/V03/213-226.pdf

$$\frac{\partial Q}{\partial t} + \frac{\partial (F - Fv)}{\partial x} + \frac{\partial (G - Gv)}{\partial y} + \frac{\partial (H - Hv)}{\partial z} = S(Q) \tag{3}$$

where $Q=[\rho, \rho u, \rho v, \rho w, e, \rho k, \rho \varepsilon]$, t is the time, F, G and H are the inviscid flux vectors and Fv, Gv and Hv are the viscous flux vectors. $S(Q)$ is the source term of k-ε turbulence model. Two equations for k-ε turbulence model are used to determine the dissipation of turbulent kinetic energy and ε the rate of dissipation and the k and ε equations, each contains nonlinear production and destruction source terms. Also ρ is the fluid density and u, v and w are the velocity components in each direction of Cartesian coordinates. While e is the total energy per unit volume, pressure p can expressed by the following state equation for ideal gas,

$$p=(\gamma - 1)[e - \tfrac{1}{2}\rho(u^2+v^2+w^2)] \tag{4}$$

The governing equations described above for compressible viscous flow are discretised by the finite volume method. A second-order, upwind Godounov scheme of Flux vector splitting method is used to discrete the inviscid flux terms and MUSCL-Hancock scheme with k-ε turbulence model is used for interpolation of variables where HLL-Reimann solver is used for shock capturing in the flow. Central differencing scheme is used in discretizing the viscous flux terms. The upstream of incident shock wave is set as inflow boundary condition, the properties and velocities of which are calculated from Rankine-Hugoniot conditions with incident shock Mach number. The downstream inflow boundary condition and wall surface are used as solid boundary conditions where the gradients normal to the surface are taken zero. All solid walls are treated as viscous solid wall boundary. For the two-equation k-ε model on solid boundaries, μ_t is set to zero.

For the purpose of numerical simulation, the computation is conducted on the model, same as experimental condition. The sectional view of adaptive girds is shown in Figure 5 (i) and Figure 5 (iii) where the upper wall of the computational domain is treated as the non-viscous symmetry boundary. The pressure contours for different positions of the reflected shock wave are shown in Figure 5 (ii) and Figure 5 (iv).

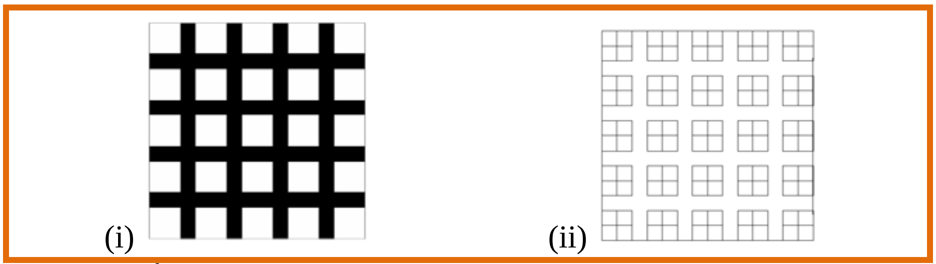

Figure 3: (i) 1/4th of turbulence-generating grid plate of 49.5 % opening area is shown; **(ii)** Configuration of numerical grids of the grid plate for computation.

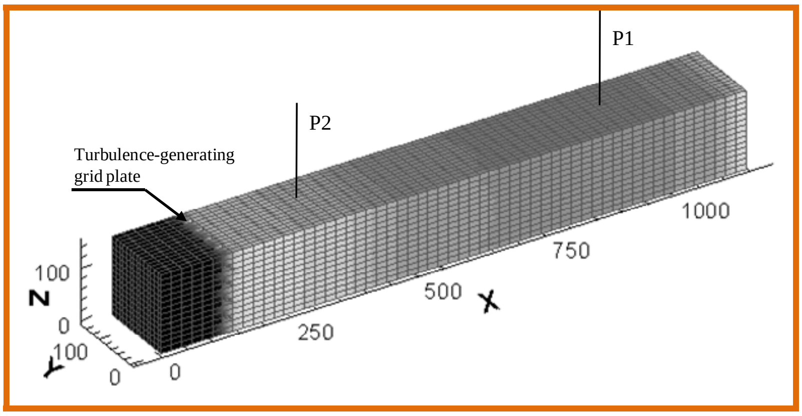

Figure 4: Three-dimensional computational domain and the position of the turbulence-generating grid plate are shown.

4. Results and Discussion

For the grid plate of 66.7 % opening area, the incident shock Mach number is 1.53 and after transmitting through the grid plate, the strength of the transmitted shock wave decreases and the measured shock Mach number is approximately 1.50. Similarly for the grid plate of 49.5 % opening area, the incident shock Mach number is 1.58 and after transmitting through the grid plate, the strength of the transmitted shock wave decreases and the measured shock Mach number is approximately 1.50. The transmitted shock wave strength is kept constant in the wake of the grid plate. It is seen that 49.5 % open area of the grid plate is less than the sonic area and 66.7 %

*Corresponding author (M. A. Jinnah). E-mail addresses: shahjin2001@yahoo.com.

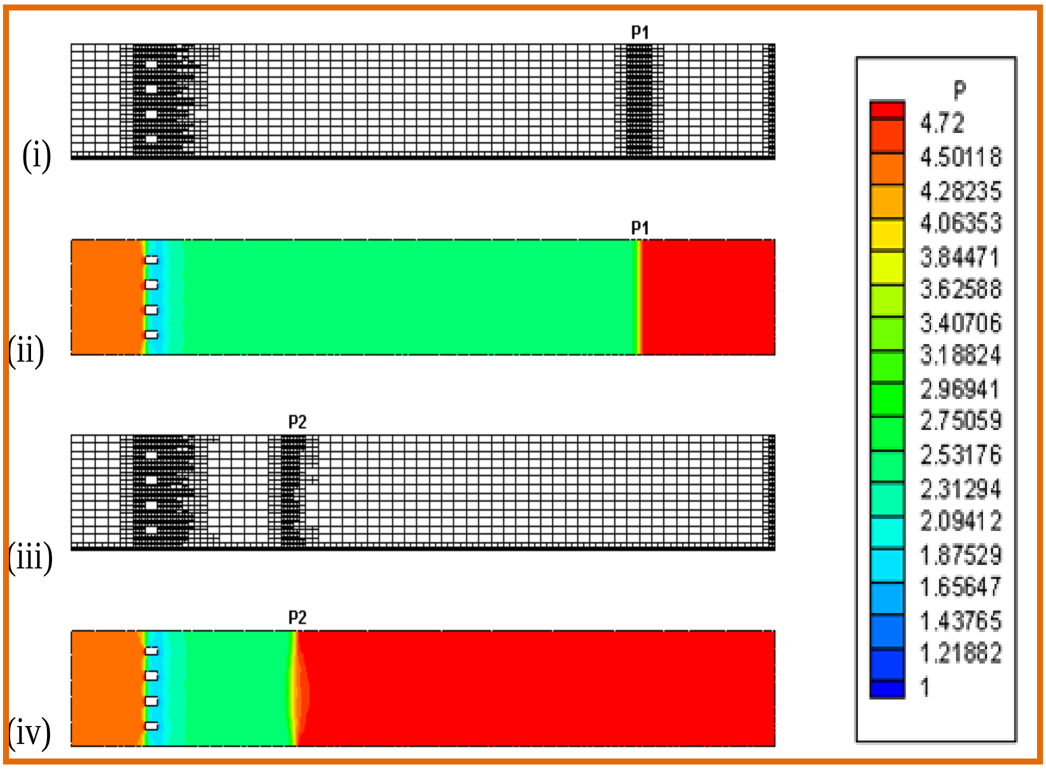

Figure 5: Sectional view of **(i)** Adaptive *ZX*-plane for the position of the reflected shock at P1; **(ii)** Pressure contour in *ZX*-plane for the position of the reflected shock at P1; **(iii)** Adaptive *ZX*-plane for the position of the reflected shock at P2; **(iv)** Pressure contour in *ZX*-plane for the position of the reflected shock at P2.

Open area is more than the sonic area. Keller and Merzkirch [7] used a perforated plate to generate the turbulent flow, which had an open area ratio 49 %. Honkan and Andreopoulous [6] used grid plate of an open area ratio 65 % in their experiments where hot-wire anemometer was used for measuring the turbulence fluctuations. Even though the turbulent field in the wake of turbulence grids is treated as homogeneous, isotropic turbulence but the turbulence intensity as well as turbulence decaying characteristics depend on the grid size and open area ratio of the grid plate. For the larger open area of the grid plate, the fully developed turbulent field in the downstream of the grids due to interaction of vortices is observed more early. For the smaller open area of the grid plate, the unsteady vortex fluctuations in the lateral direction are high which cause more flow fluctuations in the lateral direction. The turbulence decaying characteristics are obtained from the two points in the downstream of the grids and the results from these points are determined the homogeneous turbulence region. The positions P2 and P1, where pressure gauges and hot wires are placed, use to measure all turbulence parameters. Typical responses of the hot wire anemometer to transmitted and reflected shocks are shown in Figure 6, Figure 7 for the different opening areas of the grid plates. It is observed that pressure is increased across each shock wave where anemometer responses are somewhat different. The measured pressure history in the turbulent field has good agreement with theoretical equations and 4-6 percent uncertainty is observed in this pressure measurement. The mean time derivative, $\overline{\partial Q}/\partial t$ was computed for the quantity Q where Q can be any one of U or P. This derivative was computed by summing up the difference ∂Q between two successive points:

$$\frac{\overline{\partial Q}}{\partial t} = \frac{1}{n}\sum_{i=1}^{n}\frac{\Delta Q_i}{\Delta t} \tag{5}$$

The amplification of turbulence intensity is defined as the ratio of the *RMS* fluctuations in the downstream and upstream flow of the reflected shock wave.

$$\text{The amplification ratio} = \frac{[<u>/\Delta\overline{U}]_{after\_interaction}}{[<u>/\Delta\overline{U}]_{before\_interaction}} \tag{6}$$

Where the value $[<u>/\Delta\overline{U}]_{\text{after\_interaction}}$ is for the flow upstream of the reflected shock wave i.e., input to the interaction and the value $[<u>/\Delta\overline{U}]_{\text{before\_interaction}}$ is for the flow immediate downstream of the shock i.e., output of the interaction.

The turbulence intensity, $<u>/\Delta\overline{U}$ or the level of turbulence intensity in percentage are calculated in the upstream and downstream of the reflected shock wave and due to the reflected shock interaction with turbulent field, the turbulence intensity is amplified in the downstream of the reflected shock wave. The decay of turbulence intensity is observed in the downstream distance. Due to different open areas of the turbulence grid plate, the level of turbulence fluctuations also differs at the same location. In the region between the points P2 and P1, the level of turbulence fluctuations is higher for the grid plate of lower open area ratio.

After calculating the turbulence intensity from the hot wire anemometer data, it is observed that the level of the turbulence intensity is between 2.0-3.4 percent in the incident flow and 6.0-10.5 percent in the downstream flow for the grid plate of 49.5 % open area. Similarly the level of the turbulence intensity is between 2.5-3.7 percent in the incident flow and 5.5-6.1 percent in the downstream flow for the grid plate of 66.7 % open area. The

*Corresponding author (M. A. Jinnah). E-mail addresses: shahjin2001@yahoo.com.

importance of the measurements of the level of turbulence fluctuations at different locations is to relate the effect of strength of turbulence on shock/turbulence interaction. It is observed that the amplification of the turbulence fluctuations is higher close to the grids, that is for the shock wave position at P2 and decreasing at the distance far from the grids, that is for the shock wave position at P1 and the possible cause is to have more turbulence kinetic energy in the flow field at position P2. It is also observed that the maximum amplification of turbulence intensity is observed around 3.1. Even though the turbulence intensity before interaction for different grid plates have good agreement with experimental results of Honkan et al. [8] where the turbulence intensity were found 1.5-5 % but the amplification of turbulence intensity after the shock/turbulence interaction is slightly higher than the amplification, obtained by Troiler et al. [9]. The amplification of turbulence intensity was approximately 3, which was found in the experimental works of Troiler et al. [9].

The approach to isotropy of the flow was assessed by considering the skewness of the velocity fluctuations S_u. This criterion, used by Honkan and Andreopoulous [6] and Mohamed and Larue [10], is based on simple arguments concerning reflection of the downstream coordinate axis. According to this, the velocity skewness should be zero in an isotropic flow. From the results of Mohamed and Larue [10], it is observed that the uncertainty in their measurement of S_u is 0.01, these authors concluded that the position where $S_u = \pm 0.01$ is taken to be that where the flow becomes isotropic. According to this recommendation, the present flow appears to be isotropic at all downstream positions where the value of S_u is always less than 0.01.

On the other hand, the levels of RMS value of pressure fluctuations are quite different for the flow behind the reflected shock wave. It is observed that the amplification of the RMS value of pressure fluctuations is lower close to the grid plate that is for the position of port P2 and increasing at the distance far from the grid plate that is for the position of port P1. Again for the grid plate of lower open area ratio, the amplification of pressure fluctuations is lower at position P2 and higher at position P1 as compared to other types of grid plate. This may explain the slow decay of the RMS value of pressure fluctuations with downstream distance.

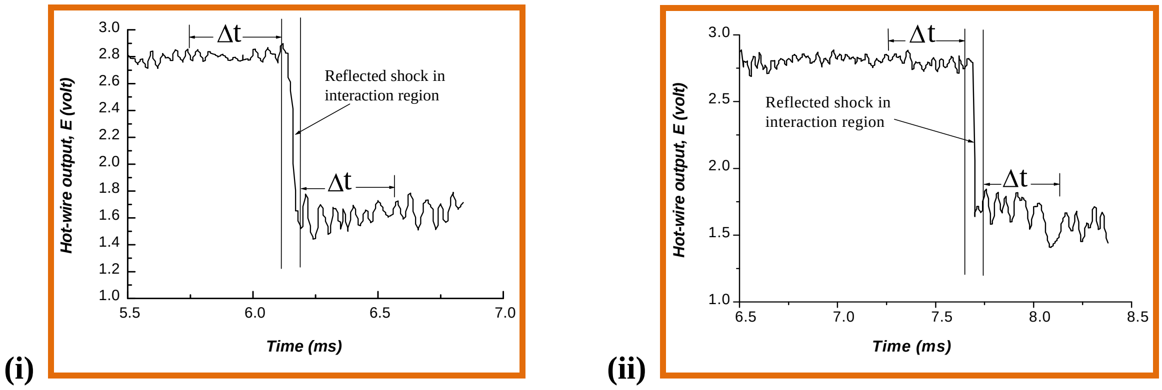

Figure 6: Hot wire output voltage profile in the upstream and downstream flow across the reflected shock for the grid plate of open area 66.7 % when the position of the reflected shock at (i) P1 and (ii) P2.

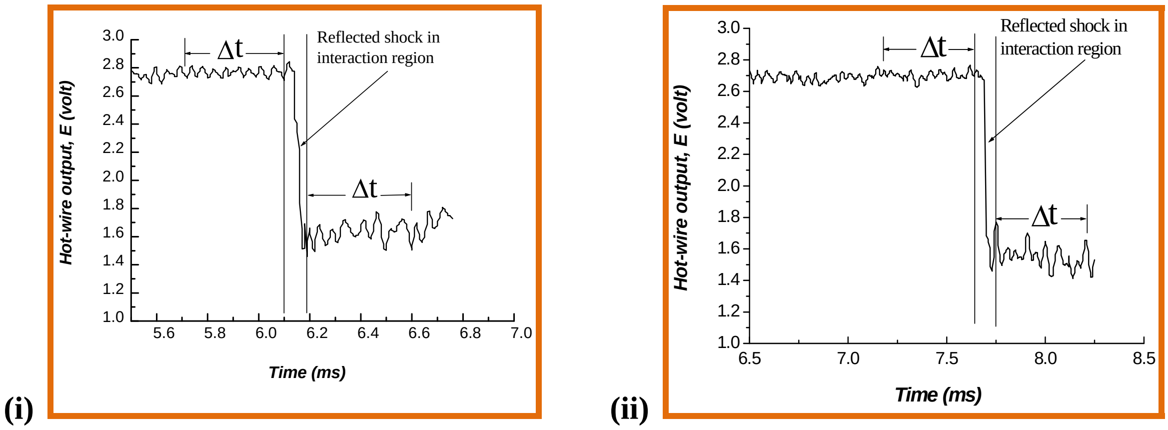

Figure 7: Hot wire output voltage profile in the upstream and downstream flow across the reflected shock for the grid plate of open area 49.5 % when the position of the reflected shock at (i) P1 and (ii) P2.

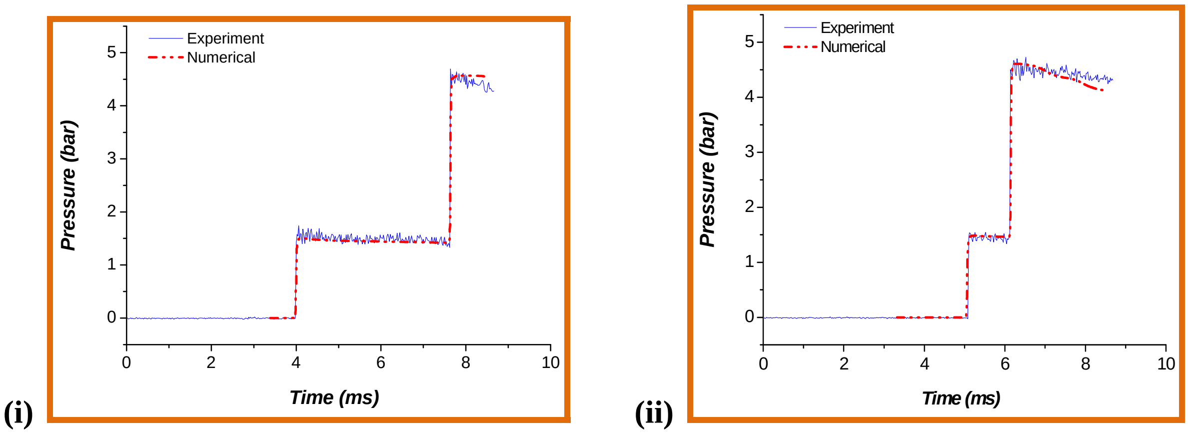

Figure 8: Simulation results of the wall pressure variations at the port points **(i)** P2; **(ii)** P1.

*Corresponding author (M. A. Jinnah). E-mail addresses: shahjin2001@yahoo.com.

(i) 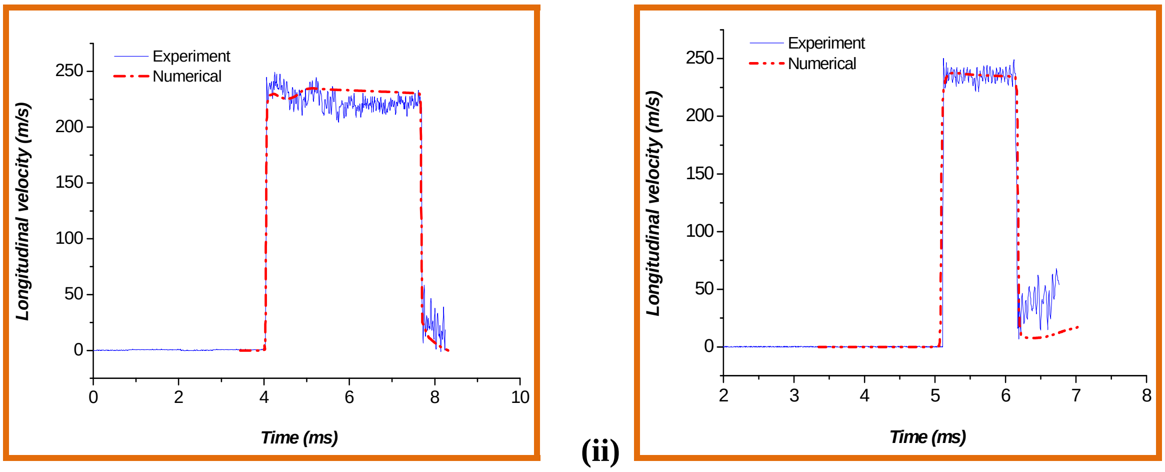

(ii)

Figure 9: Simulation results of the calibrated hot-wire output at the port points **(i)** P2; **(ii)** P1.

The wall pressures are determined for the position of P2 and P1 experimentally and compare with the numerical results, which are shown in Figure 8 (i) and (ii). It is observed that the average pressure line for the experimental pressure data simulate with numerical results properly and in some places 1-2 % deviations are observed with numerical results. Similarly the longitudinal velocities are determined after proper calibration of the hot wire data for the position of P2 and P1 experimentally and compared with the numerical results, which are shown in Figure 9 (i) and (ii). It is observed that the average longitudinal velocity line for the experimental velocity data simulate with numerical results properly and in some places 5-7 % deviations are observed with numerical results. The RMS value of velocity fluctuations and wall pressure fluctuations are also calculated at different locations of the test section experimentally and found a good agreement between numerical results and experimental results.

The present numerical code is also used to solve some turbulence parameters directly where it is difficult to get the solution in experimentally. The rate of dissipation of turbulent kinetic energy is determined numerically before and after interaction. It is observed that the rate of dissipation of TKE decreases after the shock/turbulence interaction. The levels of length scales before and after the interaction are determined numerically and it is observed that the amplification of dissipative length scale and velocity length scale are decreased in the shock/turbulence interaction.

5. Conclusion

The accuracy of the experimental results on shock/turbulence interaction depends on the response time of the instruments and also depends on the sensitivity of the hot wire anemometer. The output voltages of the hot wire are used to determine the flow velocity as well as velocity fluctuations before and after the shock/turbulence interaction and the sufficient amplification of turbulence intensity is observed after interaction. To get the corrected velocity fluctuations, proper calibrations are necessary in the same environment as the experimental setup. The uncertainty in the determination of the mean flow velocities implies an uncertainty in the calibration and thus in the velocities obtained from the hot-wire probe. The uncertainties in the measured voltages are negligible compared to the uncertainties in the calibration velocities because the voltages, used for calibration, are actually averages of a randomly fluctuating quantity. Different types of grid plates are used to change the strength of transmitted shock wave and the turbulence intensity simultaneously. So the study on different grid plates will clarify the effect of turbulence strength on shock/turbulence interaction. Numerical simulations are also conducted on the experimental results and a good agreement between numerical results and experimental results is observed.

6. References

[1] Devieve JF, Lacharme JP. (1986) A shock wave/free turbulence interaction. *Turbulent shear layer/shock wave interaction*, edited by J. Delery, Springer-Verlag, Berlin.

[2] Jacquin L, Blin E, Geffroy P. (1991) Experiments of free turbulence/shock wave interaction. *Proc. Turbulent shear flows, 8, tech Univ, Munich, Ger*. p. 1-2-1-1-2-6.

[3] Debieve FR, Gouin H, Gaviglio J. Momentum and temperature fluxes in a shock wave-turbulence interaction. *In Structure of Turbulence in heat and mass Transfer* (ed. Z. P. Zaric). Hamisphere 1982.

[4] Hesselink L, Sturtevant B. (1988) Propagation of weak shocks through a random medium. J. Fluid Mechanics; 196: 513-553.

[5] Lee S, Lele SK, Moin P. Direct numerical simulation and analysis of shock turbulence interaction. *AIAA* paper 91-0523, 1991a

[6] Honkan A, Andreopoulos J. (1992) Rapid compression of grid-generated turbulence by a moving shock wave. *Phys. Fluids* A4: 2562-72.

*Corresponding author (M. A. Jinnah). E-mail addresses: shahjin2001@yahoo.com.

[7] Keller J, Merzkirch W. (1990) Interaction of a normal shock wave with a compressible turbulent flow. *Experiments in Fluids* Vol. 8: pp. 241-248.

[8] Honkan A, Watkins CB, Andreopoulos J (1994) Experimental study of interactions of shock wave with free-stream turbulence. *Journal of Fluids Engineering*; Vol. 116: pp. 763-69.

[9] Troiler W, Duffy RE. (1985) Turbulent measurements in shock-induced flows. AIAA J. 23: 1172.

[10] Mohamed MS, LaRue JC. (1990) The decay of power law in grid-generated turbulence. *Journal of Fluid Mechanics*; Vol. 219: p-195.

Dr. Mohammad Ali Jinnah is an Associate Professor of Mechanical & Chemical Engineering Department at Islamic University of Technology (IUT). He received his B.Eng. from Bangladesh University of Engineering and Technology in 1993. He continued his PhD study at Tohoku University, Japan, where he obtained his PhD in Aeronautics & Space Engineering. Dr. Mohammad Ali Jinnah current interests involve Shock wave propagation in open Atmosphere.

Peer Review: This article has been internationally peer-reviewed and accepted for publication according to the guidelines given at the journal's website.